J. Fluid Mech. (1991), *vol.* 231, *pp.* 481–499
Printed in Great Britain

Response of the shear layers separating from a circular cylinder to small-amplitude rotational oscillations

By J. R. FILLER[1], P. L. MARSTON[1] AND W. C. MIH[2]

[1] Department of Physics, Washington State University, Pullman, WA 99164-2814, USA

[2] Department of Civil and Environmental Engineering, Washington State University, Pullman, WA 99164-3001, USA

(Received 21 October 1990 and in revised form 8 April 1991)

The frequency response of the shear layers separating from a circular cylinder subject to small-amplitude rotational oscillations has been investigated experimentally in water for the Reynolds number (*Re*) range 250 to 1200. A hot-film anemometer was placed in the separated shear layers from 1 to 1.5 diameters downstream of the cylinder, and connected to a lock-in analyser. By referencing the lock-in analyser to the cylinder oscillations, the amplitude and phase of the response to different frequency oscillations were measured directly. It is shown that rotational oscillations corresponding to cylinder peripheral speeds between 0.5 and 3% of the free stream can be used to influence the primary (Kármán) mode of vortex generation. For *Re* greater than ≈ 500, such oscillations can also force the shear-layer vortices associated with the instability of the separating shear layers. Corresponding to the primary and shear-layer modes are two distinct peaks in response amplitude versus frequency curves, and two very different phase versus frequency curves. The response of the shear layers (and near wake) in the range of Kármán frequency suggests qualitative similarities with the response of an oscillator near resonance. Forced oscillations in the higher-frequency shear-layer mode range are simply convected by the shear layers. Close to the cylinder, the shear-layer response is shown to be comparable to that of generic free shear layers studied by others.

1. Introduction

The formation and shedding of vortices from circular cylinders and other bluff bodies has been the subject of a great deal of study for over a century. It is well known, for example, that for most Reynolds numbers (*Re*) of practical importance, the so-called Kármán vortices form and are shed to the rear of the body, and may persist for some distance downstream into the wake. Reviews of the shedding phenomenon can be found in Berger & Wille (1972), Mair & Maull (1971), Wille (1974), King (1977), Blake (1986, ch. 4), and Ortel (1990). A number of researchers have studied the effects of flow-induced and forced cylinder vibration on the cylinder wake, for which King (1977), Bearman (1984), and Blake (1986) provide good reviews. In general, it has been shown that when the cylinder vibrates at or near the natural Kármán frequency, the vortex shedding synchronizes with, or locks-on to, the cylinder motion.

A comparatively smaller number of researchers have studied the effects of rotational oscillation of the cylinder. Okajima, Takata & Asanuma (1975), showed both experimentally and numerically that for *Re* 40 to 160 and 3050 to 6100, at

oscillation frequencies at or near the Kármán frequency, the vortex shedding synchronizes with the cylinder motion. Wu, Mo & Vakili (1989), have more recently done work similar to Okajima *et al.*, at Reynolds numbers 300 and 500. Taneda (1978) studied the effects of rotational oscillation at Re 30 to 300, and showed that at very high oscillation frequencies (and magnitudes), the stagnant-fluid region behind the cylinder, as well as the vortex shedding process, could be nearly eliminated. Tokumaru & Dimotakis (1991) have shown that rotational oscillation at very large magnitudes can produce significant reductions in drag on the cylinder.

A number of researchers have studied a mode of vortex shedding in the cylinder wake associated with the laminar-to-turbulent transition in the separated shear layers (Bloor 1964; Gerrard 1978; Wei & Smith, 1986; and Kourta *et al.* 1987). The work of Bloor, Gerrard and Kourta *et al.* suggests that the frequency of shedding, f_{SL}, of the shear-layer vortices can be related to the Kármán frequency, f_K, by the proportionality $f_{SL}/f_K \propto Re^{\frac{1}{2}}$, where Re is the Reynolds number based on the cylinder diameter d and free-stream speed U. Kourta *et al.* suggest that the constant of proportionality in the above relationship is approximately 0.095, i.e.

$$f_{SL}/f_K \approx 0.095 Re^{\frac{1}{2}}. \tag{1}$$

Peterka & Richardson (1969) showed that the secondary instability or mode of vortex shedding can be excited by sound. Dale & Holler (1969) showed that shear-layer vortices could be excited by vibrational oscillation of the cylinder. Their results suggest a non-dimensional frequency for the secondary instability approximated by

$$f_{SL} d/U \approx 0.02 Re^{\frac{1}{2}}. \tag{2}$$

It is shown in the present study that relatively small-amplitude rotational oscillations, in which the peripheral speed of the cylinder is only 0.5 to 3% of the free-stream speed, can couple to both modes of vortex shedding. By rotationally oscillating the cylinder at or near the natural Kármán frequency, the primary or Kármán mode of vortex shedding can be affected and, for Re greater than ≈ 500, rotational oscillation at higher frequencies can be used to force the secondary instability of the separating shear layers. (We use 'secondary instability' as synonymous with 'shear-layer instability' though some authors associate the former expression with three-dimensional effects in general shear flows.)

Figure 1 illustrates the response to small-amplitude oscillations made visible by injecting a dye into the water immediately upstream from the cylinder. The photographs show flow past both a stationary and rotationally oscillating cylinder at $Re = 925$. The shear layers separating from the stationary cylinder are relatively smooth, and wrap up into the Kármán vortices that are forming. Shear-layer vortices are not normally observed in this range, and have been reported in the literature only down to around $Re \approx 1100$ (e.g. Wei & Smith 1986). Figure 1 (*b*) shows the effect of oscillations at roughly 3 times the Kármán frequency with the maximum cylinder peripheral speed approximately 2.5% of that of the free stream (corresponding to angular displacements of about 1°). As illustrated by dye flow visualization, shear-layer vortices are generated which are qualitatively similar to those observed in a stationary cylinder wake, for example, by Wei & Smith (1986) at higher Reynolds numbers. Observations like those in figure 1 (*b*) helped to motivate the experimental arrangement used for our more quantitative study of the wake's response.

(*a*)

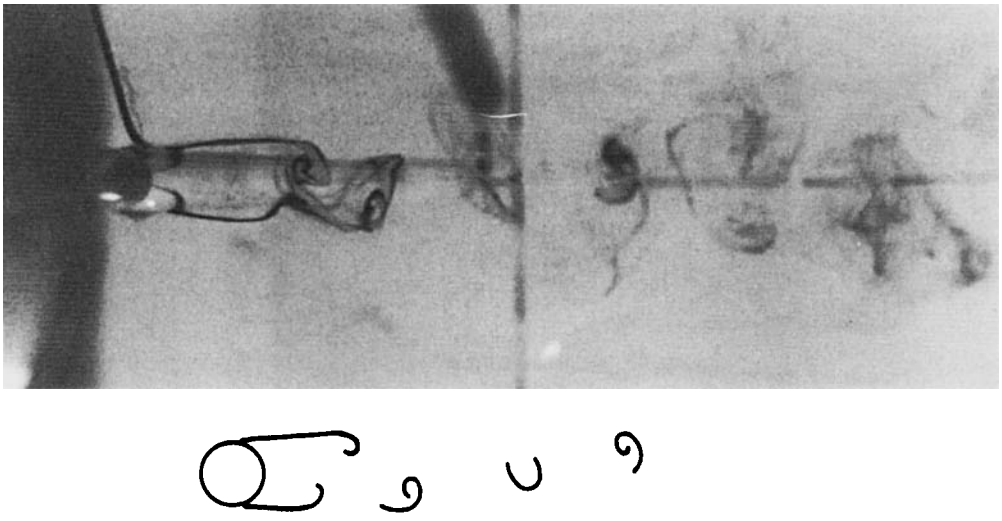

(*b*)

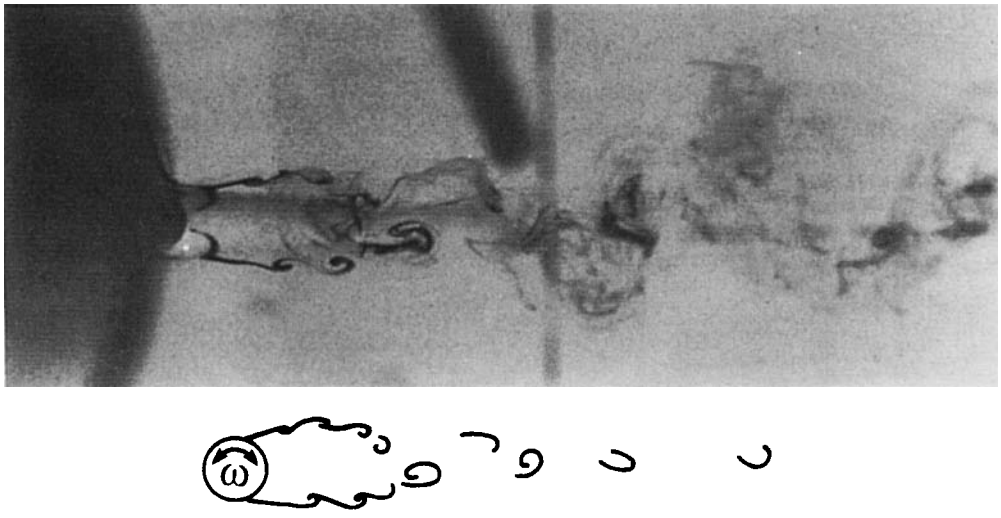

FIGURE 1. Demonstration of shear-layer (or secondary) vortex generation by rotational oscillation of the cylinder ($Re = 925$, $F = fd/U = 0.67$, $\Omega = \omega_{max} d/2U = 0.025$, $d = 1.27$ cm). (*a*) Stationary cylinder, natural shedding, (*b*) rotationally oscillating cylinder, forced shear-layer vortex shedding.

2. Experimental arrangement

To measure the response of the separated shear layers and near wake to small-amplitude rotational oscillations of the cylinder, a hot-film anemometer was placed approximately in the centre of the shear layers between 1 and 1.5 diameters downstream of separation (figure 2). The shear-layer thickness in figure 2 is

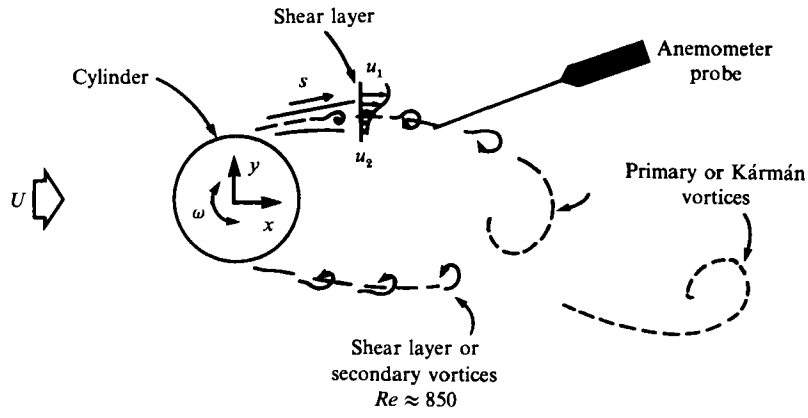

FIGURE 2. Flow past a circular cylinder subject to small-amplitude rotational oscillations (conceptual) showing shear layers and location of anemometer probe (shear-layer thickness exaggerated).

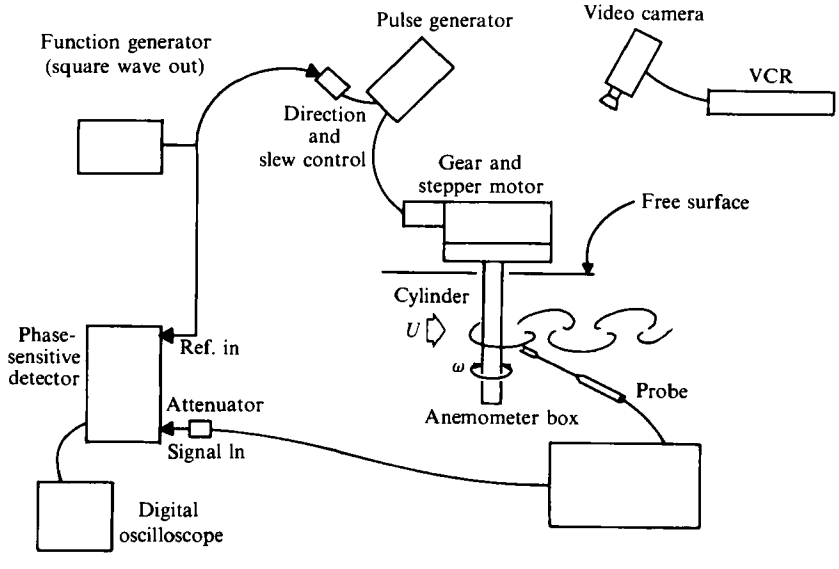

FIGURE 3. Experimental arrangement for measuring the frequency response with a hot-film probe (see text). The oscilloscope may be used to directly monitor either the fluctuations of the anemometer voltage or the output of the phase-sensitive detector.

exaggerated, being only several millimeters in the actual experiments, or 10% or less of the cylinder diameter. The anemometer was connected to a Princeton Applied Research Model 5204 lock-in analyser (also known as a phase-sensitive detector) which, in turn, was referenced to the signal generator which controlled the cylinder rotation (figure 3). In this way, direct measurements of frequency response of the shear layers or near wake were made, for both response amplitude and phase relative to the cylinder rotation.

The lock-in analyser was calibrated to give the amplitude, u', of the oscillating or fluctuating velocity signal at the reference frequency, which in this case was the fundamental forcing frequency f. Calibration of the lock-in analyser is explained in

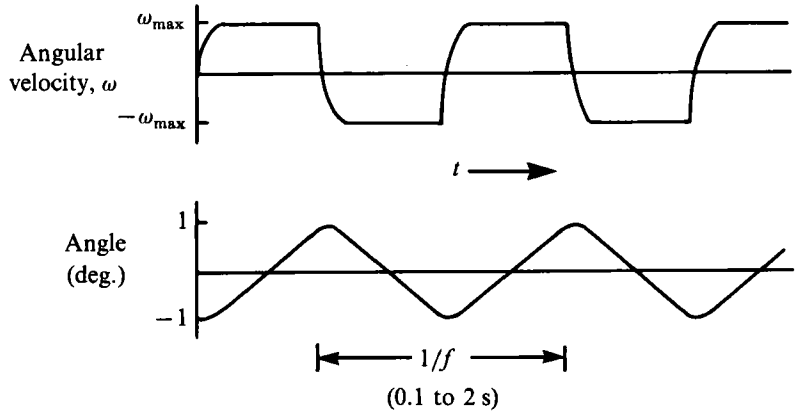

FIGURE 4. Schematic time dependence of the angular motion of the cylinder. The angular velocity is a triangle function with rounded extrema. Typically $\omega_{max} \approx 0.1$ rad/s and the maximum rotation angle $\approx 1°$.

greater detail in the Appendix. The unsteady anemometer velocity signal, $u(f,t)$, is assumed to be of the form

$$u(f,t) = u_0(f) + u'(f)\cos(2\pi ft + \phi) + u_r(f,t), \tag{3}$$

where $u_0(f)$ is the mean velocity at the particular forcing condition, u' is the amplitude of the oscillating velocity component at the frequency f of forcing, and $u_r(f,t)$ is the zero-mean residual of oscillating velocity components at frequencies other than f. As indicated by the arguments shown, each term in the decomposition on the right-hand side may depend on the choice of the forcing frequency.

Cylinder oscillation was accomplished using a pulse-driven stepper motor with a periodic change of direction controlled by the function generator. The cylinder was mounted on the axis of a rotary table which was coupled to the stepper motor through a worm gear (figure 3). The resulting cylinder motion approximated that of a triangle wave in angular position, or a square wave of clockwise and counterclockwise angular velocity (figure 4). The square-wave's rise time was much shorter than the period $1/f$. Two cylinder diameters were used: 0.95 cm and 1.27 cm. The free end of the cylinder was in each case lowered into an open-channel water flume having a width of 91 cm and length of 21 m. The cylinders were not lowered to the full depth of the flume (32 cm) to avoid flow separation at the flume bottom, providing submerged length-to-diameter ratios of 20 (1.27 cm cylinder) and 24 (0.95 cm cylinder). Finite-length, free-end, and free-surface effects were not studied in great detail, as it was assumed that they would principally affect the natural shedding, and, to a much smaller extent the flow response to cylinder oscillations close to the cylinder. Justification of this assumption is demonstrated by both the primary and shear-layer instabilities following the trend of the data from other researchers. The natural Strouhal frequencies were typically depressed by less than 5% below the measurements of Roshko (1954). The hot film was placed approximately 2.5 cm below the free surface. In the vicinity of that depth, flow visualization indicated the flow was generally two-dimensional and the variation of the incident velocity with depth was also found to be negligible. The turbulence intensity of the incident flow was measured to be less than 1%.

During each experiment, the maximum non-dimensional peripheral speed of the cylinder, $\Omega = \omega_{max} d/2U$, equal to the peripheral speed divided by that of the free

stream, was held constant, and the oscillation frequency f varied. The maximum peripheral speed of the cylinder varied from experiment to experiment, and ranged between 0.5 and 3% (Ω between 0.005 and 0.03). For comparison, oscillation amplitudes used by Tokumaru & Dimotakis (1991) correspond to values of Ω up to 16, much larger than those of the present study. Angular displacements of the cylinder were generally less than 5°. In the amplitude range studied, resulting velocity fluctuation amplitudes were found to vary roughly linearly with cylinder oscillation amplitudes (§3.2). Oscillation frequencies ranged between 0.35 and 9 Hz, corresponding to non-dimensional frequencies, fd/U, between 0.1 and 1.5, or 0.5 to 8 times that of the natural Kármán shedding frequency. The increment of frequencies tested depended on the change of response in any particular frequency range and the overall operational constraints of the flow facility. Typical runs at any particular Reynolds number took between 8 and 16 h. Experimental data are summarized in table 1.

At each oscillation frequency tested, the lock-in analyser was allowed to reach an equilibrium reading, consisting of, first, the vortex shedding process coming to equilibrium or adjusting to the new forcing condition, and, second, the lock-in analyser registering an essentially steady (or averaged) response output. The time constant used for the lock-in analyser for each test was 100 s. Consequently, the detected velocity oscillations were limited to those within a very narrow frequency band (of width ≈ 0.02 Hz) centred on f. The response amplitude represented an idealized sine-wave velocity oscillation at the frequency of reference, equation (3), essentially riding along the separated shear layer. Phase information was shown in degrees difference (or delay) between clockwise or counterclockwise motion of the cylinder and corresponding clockwise or counterclockwise roll-up of the shear layer.

3. Results

3.1. *Response amplitude and forcing frequency*

The amplitudes of velocity fluctuations resulting from the forced cylinder oscillations are shown in terms of the fluctuating component, u', divided by the free-stream speed, U, and plotted against the non-dimensional forcing frequency, $F = fd/U$. A characteristic response-amplitude curve is shown in figure 5. When the cylinder was oscillated at or near the natural Kármán frequency (Strouhal number approximately 0.2), large velocity fluctuations were observed in the shear layers, generally synchronized with the cylinder oscillations, producing the large response peak. Oscillation magnitudes in this range were as large as 30 to 50% of the free stream. Flow visualization showed that the large velocity fluctuations corresponded to the shear layer moving back and forth across the probe, alternately exposing the sensor to fast- and slow-speed shear-layer fluid.

For Reynolds numbers greater than around 500, a secondary, higher-frequency response appeared (figures 5 and 6), in addition to the one at the Kármán frequency. This response peak was typically broader and lower in amplitude than the Kármán peak, and was associated with the forcing of the smaller secondary or shear-layer vortices (figure 1). The smaller vortices typically rode along the shear layers as they rolled up into the Kármán vortices that were forming. These velocity oscillations were typically of the order of 10% or less of the free-stream velocity. In a number of experiments, a small peak was also observed at roughly twice the Kármán frequency. At forcing frequencies above and below the primary and secondary response peaks, response as indicated by the lock-in analyser died off, and in many

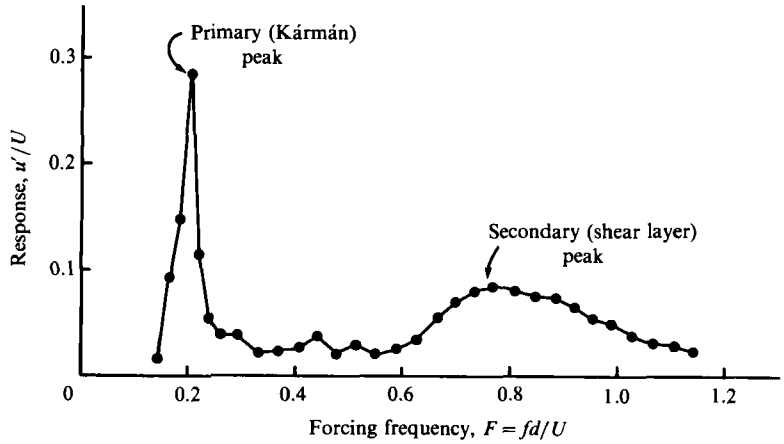

FIGURE 5. Typical frequency response curve showing the normalized response amplitude as a function of the forcing frequency for $Re = 920$, $\Omega = \omega_{max} d/2U = 0.14$, $d = 1.27$ cm, where u' is the magnitude of the oscillating component at the forcing frequency.

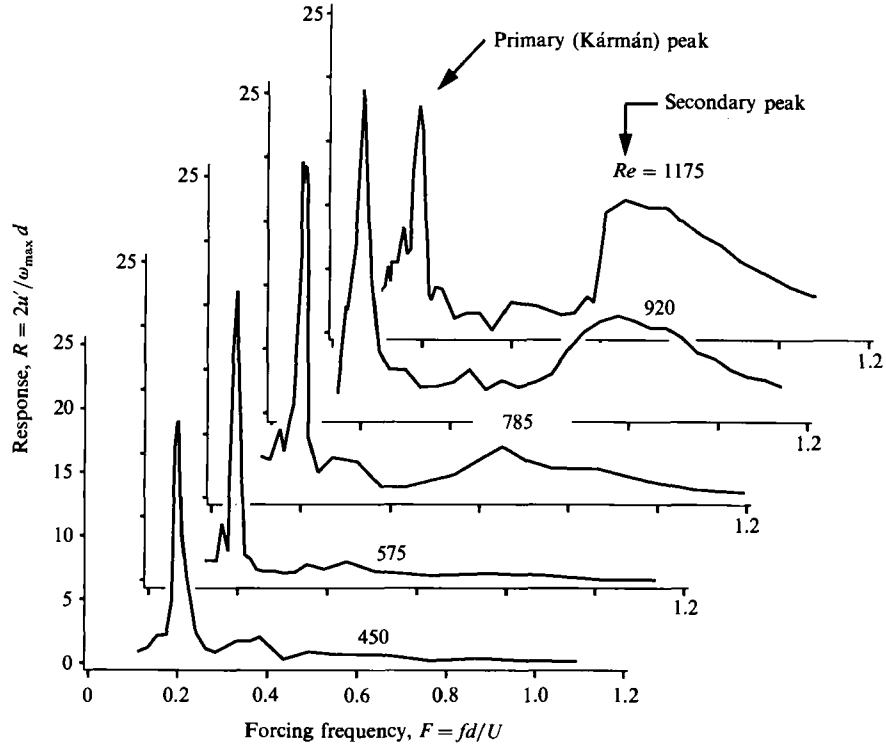

FIGURE 6. Frequency-response curves for a range of Reynolds number. The normalized response $2u'/\omega_{max} d$ is shown. The dimensionless peripheral velocity Ω is 0.019, 0.022, 0.019, 0.014, and 0.011 respectively for Re of 450, 575, 785, 920, and 1175. Notice that the relative magnitude of the normalized shear-layer response increases with Re.

cases was indistinguishable over background noise. For many forcing conditions, detected velocity oscillations were only intermittent, or possibly intermittently synchronized with the cylinder motion. Since the u'/U values shown are time-average values, the magnitudes of u'/U represent the average magnitude of the

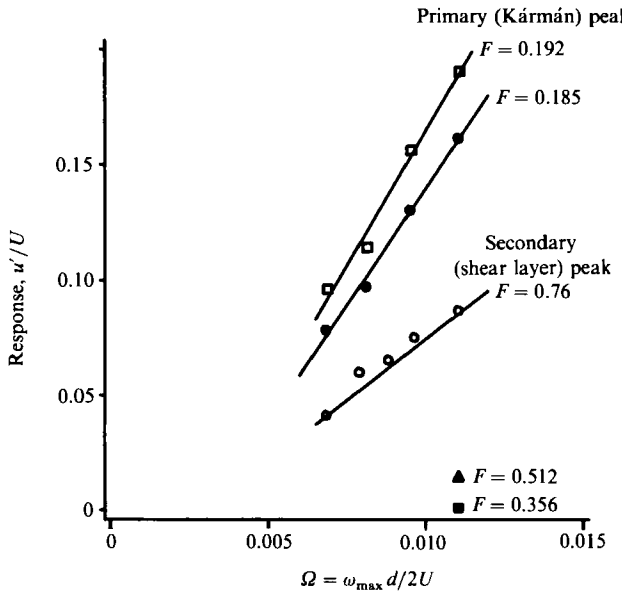

FIGURE 7. Demonstration of the approximate linearity of the response with cylinder oscillation amplitude at various forcing frequencies $F = fd/U$ ($Re = 1175$, $d = 1.27$ cm, $x/d = 1.0$). $F = 0.192$ appears to be close to, but slightly displaced from the natural shedding frequency. Under similar circumstances, measurements give a negligible ratio u'/U in the limit of vanishing Ω. The reason natural shedding is not ordinarily detected by the lock-in amplifier is because of the very small effective bandwidth of the system.

oscillations synchronized with the reference, or the fraction of time the oscillations were synchronized. These interpretations are compatible with oscilloscope records of the fluctuating voltage signal from the anemometer.

As the Reynolds number was increased above 500, the secondary peak magnitude and width generally increased. This is illustrated best in figure 6, where the response amplitude u'/U has been normalized by the forcing amplitude $\omega_{\max} d/2U$ for a number of experiments.

3.2. *Response amplitude and oscillation amplitude*

During a number of experiments, the amplitude of the response was tested against varied cylinder oscillation amplitude. Results are shown in figure 7 for $Re = 1175$. Two curves are shown for forcing in the Kármán frequency range, with one test being close to the frequency of peak response and the other at a slightly lower frequency. The third curve is in the secondary, higher-frequency response range. The curves illustrate that in both ranges the response amplitude was roughly proportional to, or linear with, the oscillation amplitude. Rough linearity of the response was important for comparison of experiments since the relative cylinder oscillation amplitudes differed between experiments, and in addition, the angular velocity $\omega(t)$ of the cylinder contained higher harmonic components. (An upper limit of the relative angular velocity amplitude of the nth odd harmonic may be found from the Fourier series coefficients of a square wave which decrease as $1/n$.) With an approximately linear response, the higher-frequency content was therefore expected to only weakly affect the phase-sensitive detector output. A linear response also allowed comparison with linear instability theory (§4). Figure 7 also shows response amplitudes at

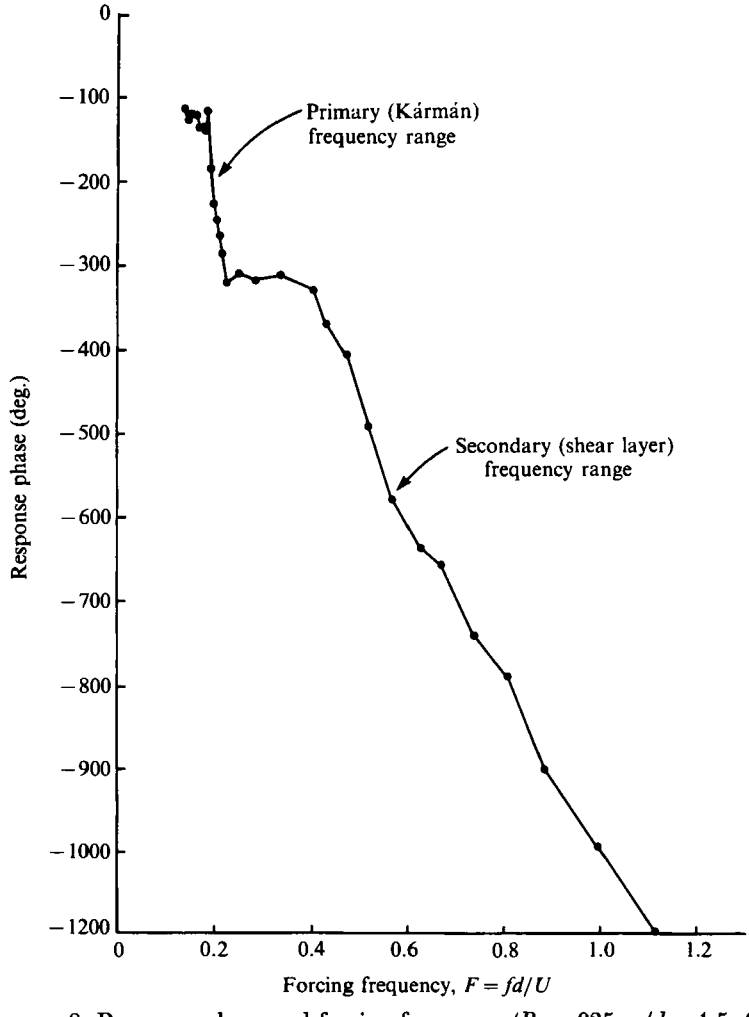

FIGURE 8. Response phase and forcing frequency ($Re = 925$, $x/d = 1.5$, $\Omega = 0.025$).

frequencies shifted far from the primary and shear-layer peaks, which, as mentioned, were very low.

In some tests the oscillation amplitudes were increased above the range shown in figure 7. In these tests the responses appeared to saturate, in qualitative agreement with the theoretical results of Goldstein & Leib (1988) for externally excited shear layers. In figure 6, the response, u'/U, divided by the cylinder oscillation magnitude, $\Omega = \omega_{\max} d/2U$, provides a normalized response value, $2u'/\omega_{\max} d$. Since $\omega_{\max} d/2$ is the maximum peripheral velocity of the cylinder, the normalized response values represent a crude amplification factor. It is interesting to note that cylinder oscillations were typically amplified by a factor of approximately 25 in the Kármán frequency range, and a factor of only 5 or 10 (or less, depending on Re) in the secondary range.

3.3. *Response phase*

At each frequency setting, the phase of the response was also recorded. Figure 8 shows a typical phase curve. Characteristic of each curve is an overall decreasing phase angle, corresponding to an increasingly delayed response relative to the forcing

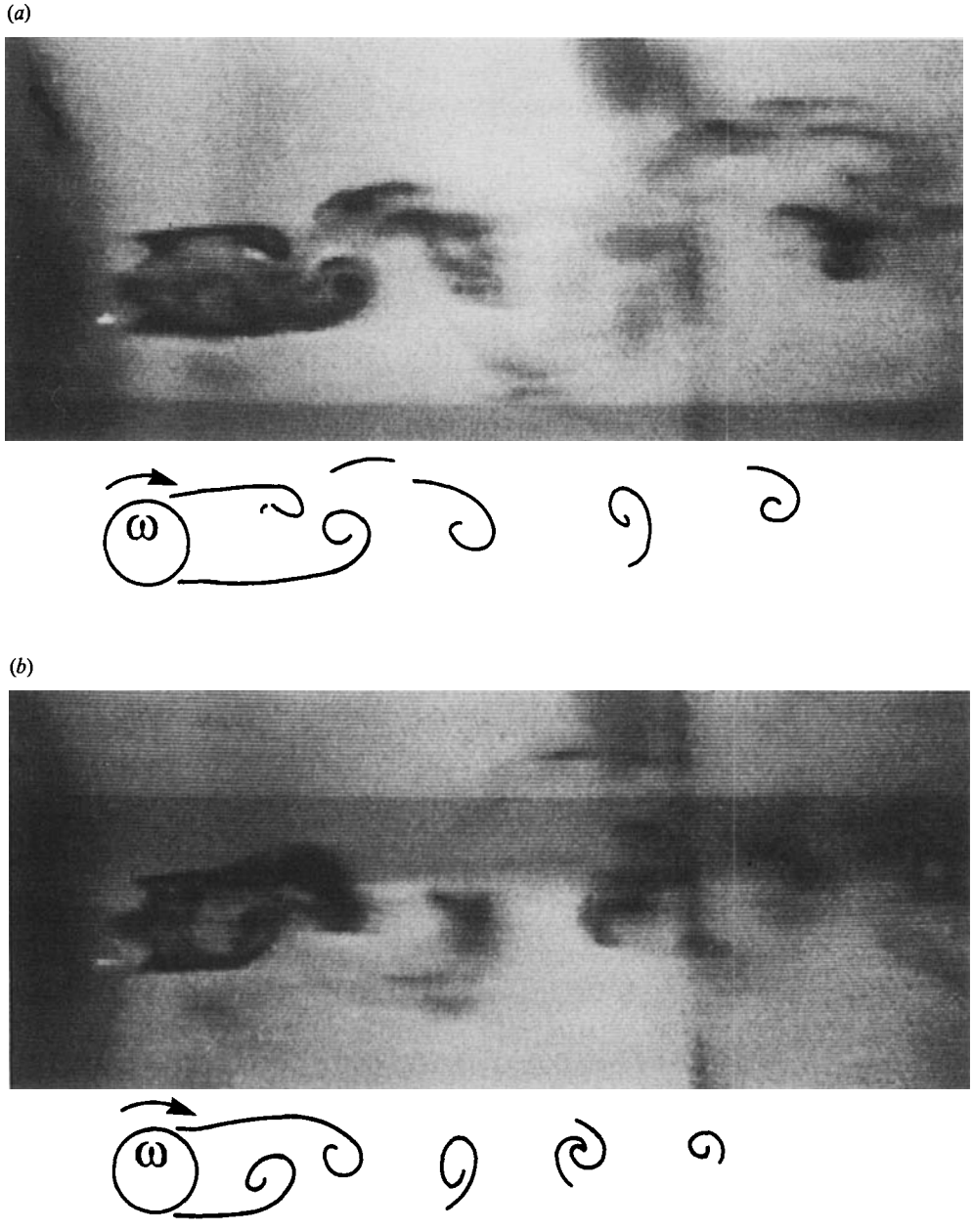

FIGURE 9. Flow visualization showing the change in phase with respect to the cylinder motion near the Kármán frequency, for $Re = 825$. In both cases the cylinder is at its maximum clockwise position. (Natural Kármán frequency $f_K d/U \approx 0.201$.) (*a*) $F = fd/U = 0.20$; (*b*) 0.22.

period. Near the natural Kármán shedding frequency, a rapid phase change (of order 180°) was observed as the Kármán frequency was crossed. This corresponded to the Kármán vortex formation essentially switching sides with respect to the cylinder motion (figure 9). As the forcing frequency was increased further, the phase varied essentially linearly with frequency, characteristic of the oscillations being convected or propagated along the separated shear layers (see §4).

For several experiments, the dependence of response amplitude and phase was tested against increasing or decreasing forcing frequency. Essentially no difference was observed for increasing or decreasing frequency for all tests, indicating a lack of significant hysteresis with forcing conditions in comparison with noise (Filler 1989).

4. Discussion

4.1. *The shear-layer instability*

The secondary higher-frequency response peaks of §3 can be compared to the response for generic free shear layers studied theoretically by others. For a mean shear-layer flow with a wave-like disturbance or perturbation, the perturbation response can be characterized by the real part of the perturbation stream function, i.e.

$$\psi'(x, y, t) = \psi'(0, y, 0)\, \mathrm{e}^{-\mathrm{i}(2\pi f t - kx)} \tag{4}$$

(for example, Monkewitz & Huerre 1982). The wave-like perturbation grows or decays in time as it travels in the x-direction with phase speed $c = 2\pi f/k'$, where k' is the real part of the complex wavenumber, $k = k' + \mathrm{i}k''$, and $2\pi f$ is the angular frequency. The spatial amplification rate in the x-direction, k'', has theoretically been shown to be frequency-dependent for the generic free shear layer (Michalke 1965), with the most amplified frequency, f^*, related to the mean shear-layer speed $\bar{u}$, and momentum thickness θ, by

$$f^*\theta/\bar{u} = 0.032, \tag{5}$$

where the momentum thickness of the shear layer is defined as

$$\theta = \frac{1}{(u_1 - u_2)^2} \int_{-\infty}^{\infty} (u_1 - u)\,(u - u_2)\,\mathrm{d}y,$$

u_1 and u_2 being the shear-layer fast and slow speeds, respectively (Monkewitz & Huerre 1982 and Ho & Huerre 1984, laminar shear layers). The saturated end-product vortices in experimentally perturbed shear layers have been found to evolve at essentially the same frequency as f^*, and, further, vortices forming in unperturbed shear layers are found to have a most probable frequency, f_{m}, of roughly this same value (Ho & Huang 1982 and Ho & Huerre, 1984). The theoretical studies also indicate that perturbations with frequencies up to approximately twice f^* are amplified in the free shear layer.

Roshko (1954), Churchill (1988, pp. 337–339), and others, relating the flow outside the boundary layer to the base pressure behind the cylinder, suggest that the typical value of the flow speed outside the boundary layer prior to separation is around $1.4U$. Coarse velocity measurements as a part of this investigation (Filler 1989) indicate that this value is approximately correct for the outer- or fast-stream speed of the shear layer, once it separates from the cylinder and for up to one or more diameters downstream of separation. Assuming a relatively stagnant (average) flow inside the separating boundary layers, the mean speed $\bar{u}$ of the resulting shear layers may be approximated by $\frac{1}{2}(1.4U + 0)$, or $0.70U$.

Boundary-layer computations in Schlichting (1979, p. 216) suggest that the momentum thickness θ of the boundary layers prior to separation can be approximated by $\theta \approx C d Re^{-\frac{1}{2}}$, where C is approximately unity. Coarse measurements as a part of the present study (Filler 1989) indicate that the separated shear layer has approximately this same thickness to 1 to 1.5 diameters downstream of separation. C. H. K. Williamson (1989, personal communication) has taken measurements of the

1	2	3	4	5	6	7	8
Re	f' (Hz)	d (cm)	U (cm/s)	$\frac{f'd\,Re^{-\frac{1}{2}}}{0.70U}$	$\partial\phi/\partial f$ (deg./Hz)	x/d	$-(\partial\phi/\partial f)(\nu/2\pi xd)$ (10^{-3})
300	—	0.95	2.93	—	−314	1.5	6.04
375	—	0.95	3.66	—	−208	1.5	3.93
450	—	0.95	4.36	—	−209	1.5	3.93
510	(*a*)	1.27	3.72	(*a*)	−237	1.5	2.44
575	1.75	1.27	5.03	0.026	−265	1.5	2.99
630	(*a*)	0.95	6.25	(*a*)	−105	1.2	2.59
690	2.60	1.27	5.27	0.034	−208	1.5	2.31
710	2.75	1.27	5.33	0.035	−227	1.5	2.49
745	2.50	1.27	5.64	0.029	−197	1.5	2.18
760	2.60	1.27	5.76	0.030	−191	1.5	2.11
785	3.00	1.27	5.85	0.033	−178	1.3	2.32
815	3.15	1.27	6.09	0.033	−223	1.5	2.43
875	3.30	1.27	6.95	0.029	−162	1.5	1.88
920	4.23	1.27	6.92	0.037	(*c*)	1.5	(*c*)
925	3.65	1.27	7.41	0.029	−165	1.5	1.92
990	4.25	1.27	7.77	0.032	−116	1.0	1.98
1050	4.50	1.27	7.86	0.032	−145	1.5	1.60
1175	4.77	1.27	8.93	0.028	−119	1.0	1.97
				average[b] 0.031			

(*a*) The frequency of peak response was unclear or not apparent in this experiment.
(*b*) Compare with 0.032 for theoretical studies of generic free shear layers (for example, Ho & Herre 1984).
(*c*) Data not recorded for this experiment.

TABLE 1. Frequency f' of the maximum response for the shear-layer instability, phase derivative with frequency, and other experimental data

shear-layer vorticity thickness one diameter downstream of separation that suggest a similar value of unity for C.

Using the above relations for the separated-shear-layer mean speed and momentum thickness, the frequencies of maximum response, f', of the present study were compared to theoretically predicted frequencies of greatest amplification, e.g. the values of $f'\theta/\bar{u}$ compared with 0.032 of Ho & Huerre (1984), where $f'\theta/\bar{u}$ may be approximated by

$$f'\theta/\bar{u} \approx f'd\,Re^{-\frac{1}{2}}/0.70U. \tag{6}$$

Table 1 (column 5) shows the observed non-dimensional frequencies of maximum response using (6). The agreement with the theoretical value of 0.032 is acceptable. Furthermore, it was observed (for Re greater than $\approx$ 500) that positive response to rotational oscillation of the cylinder continued up to frequencies of roughly $2f'$, which is what would be expected in the generic shear-layer analogy. These results suggest, therefore, that the shear layers separating from a circular cylinder are indeed comparable to generic free shear layers (prior to their roll-up into the Kármán vortices), and, that the frequencies of greatest response are approximated by the theoretical frequency of maximum amplification rate for generic free shear layers.

The frequencies of maximum response f' of the present study were also divided by the natural Kármán shedding frequencies f_K, and compared to the natural shear-layer vortex shedding frequencies from other researchers. The agreement with the

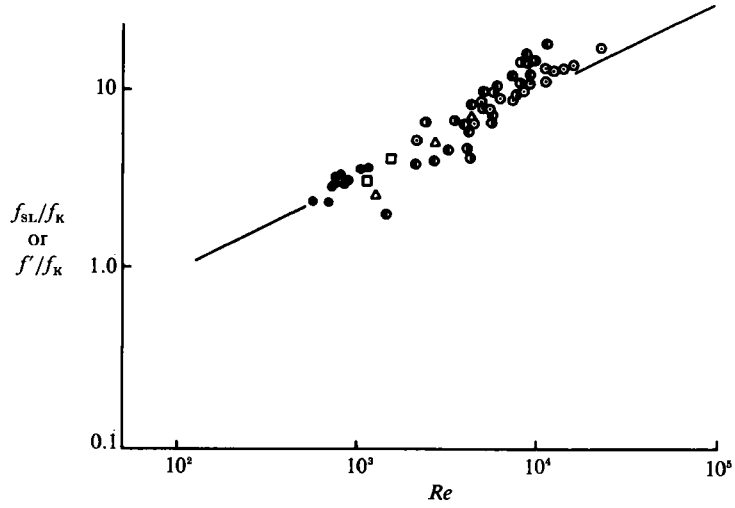

FIGURE 10. Comparison of normalized frequencies of maximum response from the present study (solid circles) with natural secondary shedding frequencies found by other authors for a range of Reynolds numbers: △, Bloor (1964); □, Gerrard (1978); ◑, ◐, Wei & Smith (1986); ⊙, Kourta *et al.* (1987). The line is given by equation (1).

present data and equation (1) representing the trend of the data from Kourta *et al.* is good (figure 10), suggesting that the trend of the data from others continues down to around 500. Therefore, the frequencies of maximum response in the present (forced) study are also comparable to the naturally shedding shear-layer frequencies (f_{SL}) observed by Bloor, Gerrard, and others at higher Reynolds numbers, although naturally shedding shear-layer vortices have not readily been observed or reported by others for Reynolds numbers much below 1100.

Rearrangement of the above relationships also allows a prediction of the frequencies of greatest response for the shear-layer vortex shedding frequency, and likewise a prediction equation for the naturally occurring secondary or shear-layer vortices. Equation (6), with $f^*\theta/\bar{u} \approx f'\theta/\bar{u} \approx 0.032$, gives, in terms of a non-dimensional shedding frequency,

$$f_{SL}d/U \approx f'd/U \approx 0.022Re^{\frac{1}{2}}. \tag{7}$$

Measured values of $f'd/U$ are shown in figure 11 along with (7). A least-squares fit of the data gives $f'd/U = 0.023Re^{0.495}$. Both the least-squares fit and the more theoretically motivated equation (7) are in good agreement with measured values of Dale & Holler (1969, equation (2)) and other researchers (assuming $f_K d/U \approx 0.20$ in the other studies).

4.2. *Response phase*

In the range of the shear-layer instability, the phase variation with oscillation frequency was roughly linear. Considering again a disturbance of the form of (4), the phase of the disturbance, ϕ, may be expressed in radians as, $\phi = -k's$, or $\phi = -2\pi fs/c$, where s is the propagation distance along the shear layer (figure 2), and c is the phase speed. In the Reynolds-number range of the present study, separation occurs approximately halfway between the forward and rear stagnation points, i.e. at $x \approx 0$ (see for example, Churchill 1988, pp. 333–334). Assuming that the shear layers are roughly parallel to the wake axis prior the primary vortex roll-up, then $s \approx x$. Using for c the mean shear-layer speed $\bar{u}$ (which is supported by experimental

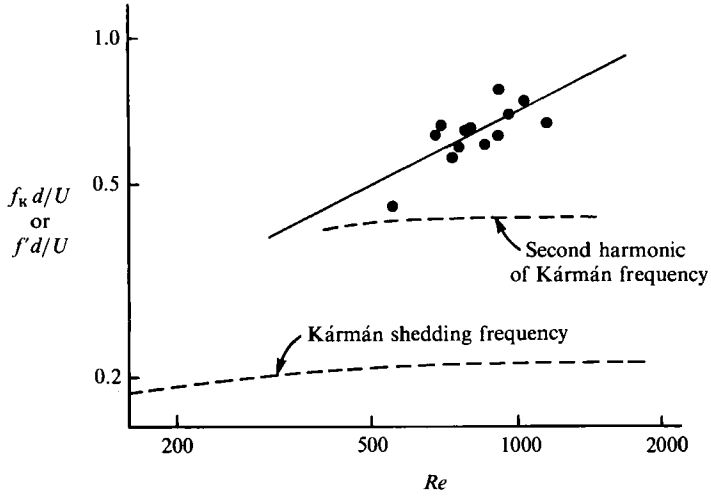

FIGURE 11. The points are the non-dimensional frequencies of maximum response associated with the secondary shedding mode as a function of Reynolds number. The solid line is given by equation (7). For comparison, the lower dashed curve represents Roshko's (1954) shedding frequencies for Kármán vortex shedding. The upper dashed curve is twice the natural Kármán frequency; note that it approaches the line from equation (7) at a Reynolds number near which the shear-layer vortex shedding becomes difficult to observe.

evidence for free shear layers, Monkewitz & Huerre 1982 and Ho & Huerre 1984), the phase of the forced oscillations may be approximated $\phi \approx -2\pi f x/\bar{u}$. The derivative of the phase with respect to forcing frequency, $\partial\phi/\partial f$, is thus,

$$\partial\phi/\partial f = -2\pi s/c \approx -2\pi x/\bar{u}. \qquad (8a,b)$$

Measured values of $\partial\phi/\partial f$ are shown in table 1 (column 6) for a number of tests. It should be pointed out that while the response amplitude values for the secondary instability were nearly indistinguishable from the background for $Re < 500$, the response phase could be measured for Reynolds below 500. The measured values may be compared with predictions by noting the following relationship which follows from (8a):

$$Re^{-1} = -\kappa(\partial\phi/\partial f)(\nu/2\pi x d), \qquad (9)$$

where $\kappa = cx/Us$ is a constant and ν is kinematic viscosity. Assuming $x \approx s$ and $c \approx \bar{u} \approx 0.70U$ suggests $\kappa \approx 0.70$.

Values of $-(\partial\phi/\partial f)(\nu/2\pi x d)$ are plotted against Re^{-1} in figure 12. A least-squares fit of the data (constrained to pass through the origin) suggests a value for κ of 0.60. The difference from 0.70 (approximately 15%) is due at least in part to the underestimation of s by x (figure 2). General scatter is likely to be due to the imprecision in the measurement of x (Filler 1989). The straight-line trend of the data, however, does suggest that the forced oscillations in the secondary higher-frequency regime behave as waves simply propagated along the shear layer at the mean speed $\bar{u}$, prior to roll-up of the shear layers into the larger Kármán vortices.

4.3. *Response close to the natural Kármán shedding frequency*

Rotational oscillation near the natural Kármán frequency f_K generally enhanced the natural Kármán vortex shedding. Flow visualization indicated that vortex formation was more distinct and closer to the cylinder (Filler 1989) similar to the results of others using vibrational oscillation (e.g. Griffin & Ramberg 1974). As the natural Kármán frequency was crossed, the first vortex formed changed sides with respect

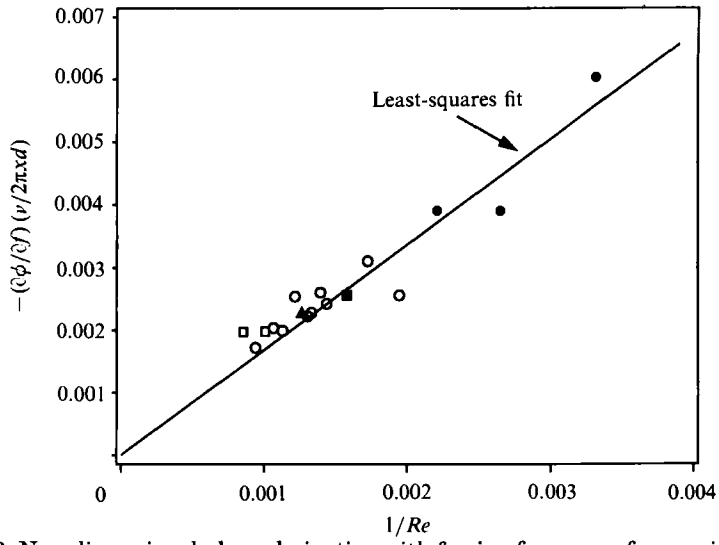

FIGURE 12. Non-dimensional phase derivative with forcing frequency for varying cylinder size and propagation distance. ■, $d = 0.95$ cm, $x/d = 1.2$; ●, $d = 0.95$ cm, $x/d = 1.5$; □, $d = 1.27$ cm, $x/d = 1.0$; ▲, $d = 1.27$ cm, $x/d = 1.3$; ○, $d = 1.27$ cm, $x/d = 1.5$. The phase ϕ is measured in radians.

to the cylinder motion, corresponding to a phase change (or jump) of approximately 180° (figure 8). At forcing frequencies slightly lower than the Kármán frequency, the rotation of the cylinder and roll-up of the first vortex formed were in the same direction. As f_K was crossed, the first vortex formed changed sides with respect to the cylinder motion (figure 9), and rolled up in the opposite direction to the corresponding cylinder rotation. A similar 180° phase jump has been observed by others for forced vibration of the cylinder perpendicular to the free stream (Zdravkovich 1982 and Ongoren & Rockwell 1988). The large response and rapid phase change for f near f_K suggest that the near wake and shear layers respond to weak rotational oscillations in a way which is roughly analogous to a linear mechanical oscillator near resonance. The absence of significant hysteresis mentioned in §3.3 is consistent with this analogy.

5. Conclusions and closing remarks

Using a lock-in analyser connected to a hot-film anemometer placed in the shear layers separating from a circular cylinder, both the amplitude and phase of the frequency response of the cylinder near wake were measured directly. The present study shows first of all that small-amplitude rotational oscillations of the cylinder, of the order of 1–3% of the free-stream speed, couple with both the Kármán and shear-layer vortex shedding modes. The oscillations were particularly effective in forcing the shear-layer mode. Close to the cylinder, and for frequencies significantly above the natural Kármán shedding frequency, the shear layers respond in a way compatible with what would be expected for free shear layers. The response of the shear layers to rotational oscillation suggests that for small amplitudes the oscillations act to provide weak antisymmetric perturbations to the flow, and thus allowed comparisons with theoretical results of others for generic free shear layers. Figure 1 (*b*) and other observations show that the resulting shear-layer vortices form antisymmetrically whereas naturally occurring shear-layer vortices have been

reported to form symmetrically (Gerrard 1978). The frequency of maximum response of the shear layers to oscillation of the cylinder corresponds to the frequency of theoretical maximum amplification rate obtained by others, and the resulting oscillations in the shear layer are convected at roughly the mean shear-layer speed. The present study also shows that using the most amplified frequency predicted by others for free shear layers, and estimates of the separated shear-layer mean speed and momentum thickness, the shedding frequency of naturally occurring shear-layer vortices or transition waves can also be estimated.

When the fundamental forcing frequency f is near the natural Kármán shedding frequency f_K, the observed response may be more difficult to model. The range of Re studied was well above the critical Reynolds number threshold Re_c for the natural shedding of vortices. Typical reported values for Re_c lie below 50; however, they depend on the cylinder's end conditions and aspect ratio (Lee & Budwig 1991). Linear resonance responses to flow perturbations have been reported by Provansal, Mathis & Boyer (1987) when $Re < Re_c$. Huerre & Monkewitz (1990, §§6 and 7) and Oertel (1990) have reviewed the implications of hydrodynamic stability theory for the shedding of Kármán vortices. A number of recent experiments (e.g. Olinger & Sreenivasan 1988; and Strykowski & Sreenivasan 1990) have concentrated on the range of Re close to, but slightly above, Re_c where the relevant instabilities are perhaps more subject to a quantitative analysis than for the range between 250 and 1200 of the present experiments. In the supercritical region close to Re_c, the wake acts like a nonlinear system having a limit cycle corresponding to Kármán vortex shedding (Olinger & Sreenivasan 1988; Karniadakis & Triantafyllou 1989). Limit-cycle behaviour is also implicit in various phenomenological models of vortex shedding. For example, the model of Iwan & Blevins (1974) gives a Van der Pol oscillator even for the case of a stationary cylinder. As Re is increased sufficiently above Re_c, Sreenivasan (1985) has given evidence that the dynamics of the wake appears to become that of a chaotic system for which the dimensionality generally increases with Re.

The implications of the nonlinear dynamics of the wake on the interpretation of our response measurements (figures 5–8) have not been fully explored for f in the vicinity of f_K. These measurements are primarily sensitive to velocity oscillations at (or very close to) the fundamental forcing frequency f. This frequency selectivity is because the bandwidths of the amplitude measurements were small as a consequence of the long integration time (100 s) of the lock-in amplifier. It was noted in §4.3 that the amplitude and phase measurements display an approximate similarity with the response of a linear harmonic oscillator having a natural frequency of f_K. A possible explanation is that the rotational oscillations may be only coupled weakly to the Kármán shedding mode because of the low values for the dimensionless peripheral velocity Ω. Limit-cycle oscillators, when only weakly driven at a frequency slightly shifted from the natural frequency, can display a combination of responses associated with the natural and driven frequencies (Nayfeh & Mook 1979). Our measurements may correspond to the driven-frequency component of such a system. A detailed explanation of the observations for f in the vicinity of f_K would be aided by higher resolution measurements than possible with the present apparatus. The response close to f_K, with the present apparatus, may have been affected by the aspect ratio of our cylinders and by possible oblique shedding of the Kármán vortices. Nevertheless, it would be helpful to carry out a detailed two-dimensional numerical simulation, analogous to simulations given by Karniadakis & Triantafyllou for the response to an oscillation added to the free-stream velocity.

This work was partially supported by the Office of Naval Research contract N00014-85-C-0141.

Appendix. Calibration of the lock-in analyser

Calibration of the lock-in analyser (phase-sensitive detector) was necessary to reduce the oscillating anemometer voltage to a corresponding oscillating velocity, equation (3) of §2. The lock-in analyser measured only the magnitude E' and the phase ϕ of the anemometer voltage oscillating at the frequency of reference. The total anemometer voltage is assumed to be of the form

$$E(t) = E_0(f) + E'(f)\cos(2\pi f + \phi) + E_r(f,t), \tag{A 1}$$

corresponding to the assumed velocity signal of equation (3). Here $E_r(f,t)$ is a zero-mean residual of oscillating voltage components at frequencies other than f. The lock-in analyser output voltage E_L is given by $K_L E'$, where the coefficient K_L was determined by application of a known voltage to the input of the analyser. The oscillating voltage, E', was then related to the corresponding oscillating velocity component through the anemometer calibration curve, i.e.

$$u' = E'\,\partial u/\partial E \tag{A 2}$$

(assuming small oscillations) where $\partial u/\partial E$ is the slope of the anemometer calibration curve at fixed temperature. Owing to the nonlinearity of the anemometer response, however, $\partial u/\partial E$ varied as the average flow speed past the probe varied, which occurred between experiments and often with changing forcing conditions (such as varying the cylinder oscillation frequency). These changes were the most pronounced at higher Reynolds number where the shear layers were thinner, and where slight relative movement of the average shear-layer position exposed the probe to either faster or slower mean speed fluid.

To compensate for the changing position or mean speed of the shear layer, the mean anemometer voltage E_0 (corresponding to the mean speed in (A 1)) was recorded at each frequency. The oscillating velocity signal was then computed based on the slope $\partial u/\partial E$ at the appropriate mean voltage E_0. As shown in Filler (1989), however, such adjustment did not qualitatively change the results or shapes of the inferred frequency response curves in comparison with curves for which the dependence of $\partial u/\partial E$ on f was ignored. The adjusted response curves appeared, however, to have an overall reduction of noise.

Finally, it should be pointed out that the oscillating component of the voltage signal was not always small as assumed in the above small-signal theory. Near the primary response peak, inferred velocity oscillations (peak-to-peak) were in some cases of the order of the free-stream speed itself. It was found, however, that using the small-signal approximation, (A 2) adequately represented the relative response for various forcing frequencies, and thus allowed the identification of the primary and secondary response peaks.

REFERENCES

Bearman, P. W. 1984 Vortex shedding from oscillating bluff bodies. *Ann. Rev. Fluid Mech.* **16**, 195–222.

Berger, E. & Wille, R. 1972 Periodic flow phenomena. *Ann. Rev. Fluid Mech.* **4**, 313–340.

Blake, W. K. 1986 *Mechanics of Flow-Induced Sound and Vibration*. Academic.

Bloor, M. S. 1964 Transition to turbulence in the wake of a circular cylinder. *J. Fluid Mech.* **19**, 209–304.

CHURCHILL, S. W. 1988 *Viscous Flows.* Butterworth.

DALE, J. R. & HOLLER, R. A. 1969 *Secondary Vortex Generation in the Near Wake of Circular Cylinders.* US Naval Air Development Center, Warminster, Pennsylvania.

FILLER, J. R. 1989 Response of the shear layers separating from a circular cylinder to small amplitude rotational oscillation. Ph.D. dissertation, Washington State University.

GERRARD, J. H. 1978 The wakes of cylindrical bluff bodies at low Reynolds number. *Phil. Trans. R. Soc. Lond.* A **288**, 351–382.

GOLDSTEIN, M. E. & LEIB, S. J. 1988 Nonlinear roll-up of externally excited free shear layers. *J. Fluid Mech.* **191**, 481–515.

GRIFFIN, O. M. & RAMBERG, S. E. 1974 The vortex-street wakes of vibrating cylinders. *J. Fluid Mech.* **66**, 553–576.

HO, C. M. & HUANG, L. S. 1982 Subharmonics and vortex merging in mixing layers. *J. Fluid Mech.* **119**, 443–473.

HO, C. M. & HUERRE, P. 1984 Perturbed free shear layers. *Ann. Rev. Fluid Mech.* **16**, 365–424.

HUERRE, P. & MONKEWITZ, P. A. 1990 Local and global instabilities in spatially developing flows. *Ann. Rev. Fluid Mech.* **22**, 473–537.

IWAN, W. D. & BLEVINS, R. D. 1974 A model for vortex induced oscillation of structures. *Trans. ASME* E: *J. Appl. Mech.* **41**, 581–586.

KARNIADAKIS, G. E. & TRIANTAFYLLOU, G. S. 1989 Frequency selection and asymptotic states in laminar wakes. *J. Fluid Mech.* **199**, 441–469.

KING, R. 1977 A review of vortex shedding research and its application. *Ocean Engng* **4**, 141–171.

KOURTA, A., BOISSON, H. C., CHASSAING, P. & MINH, H. H. 1987 Nonlinear interaction and the transition to turbulence in the wake of circular cylinder. *J. Fluid Mech.* **181**, 141–161.

LEE, T. & BUDWIG, R. 1991 A study of the effect of aspect ratio on vortex shedding behind circular cylinders. *Phys. Fluids* A **3**, 309–315.

MAIR, W. A. & MAULL, D. J. 1971 Bluff bodies and vortex shedding – a report on Euromech 17. *J. Fluid Mech.* **45**, 209–224.

MICHALKE, A. 1965 On spatially growing disturbances in an inviscid shear layer. *J. Fluid Mech.* **23**, 251–544.

MONKEWITZ, P. A. & HUERRE, P. 1982 Influence of the velocity ratio on the spatial stability of mixing layers. *Phy. Fluids* **25**, 1137–1143.

NAYFEH, A. H. & MOOK, D. T. 1979 *Nonlinear Oscillations.* John Wiley & Sons Inc.

OERTEL, H. 1990 Wakes behind blunt bodies. *Ann. Rev. Fluid Mech.* **22**, 539–564.

OKAJIMA, A., TAKATA, H. & ASANUMA, T. 1975 Viscous flow around a rotationally oscillating circular cylinder. *Inst. Space and Aero. Sci. Rep.* 532. University of Tokyo.

OLINGER, D. J. & SREENIVASAN, K. R. 1988 Nonlinear dynamics of the wake of an oscillating cylinder. *Phys. Rev. Lett.* **60**, 797–800.

ONGOREN, A. & ROCKWELL, D. 1988 Flow from an oscillation cylinder. Part 1. Mechanism of phase shift and recovery in the near wake. *J. Fluid Mech.* **191**, 197–223.

PETERKA, J. A. & RICHARDSON, P. D. 1969 Effects of sound on separated flows. *J. Fluid Mech.* **37**, 265–287.

PROVANSAL, M., MATHIS, C. & BOYER, L. 1987 Bérnard–von Kármán instability: transient and forced regimes. *J. Fluid Mech.* **182**, 1–22.

ROSHKO, A. 1954*a* On the development of turbulent wakes from vortex streets, *NASA Rep* 1191.

ROSHKO, A. 1954*b* A new hodograph for free-streamline theory, *NASA Tech. Note* 3168.

SCHLICHTING, H. 1979 *Boundary-Layer Theory.* McGraw-Hill.

SREENIVASAN, K. R. 1985 Transition and turbulence in fluid flows, and low-dimensional chaos. In *Frontiers of Fluid Mechanics* (ed. S. H. Davis & J. L. Lumley), pp. 41–67. Springer.

STRYKOWSKI, P. J. & SREENIVASAN, K. R. 1990 On the formation and suppression of vortex 'shedding' at low Reynolds numbers. *J. Fluid Mech.* **218**, 71–107.

TANEDA, S. 1978 Visual observations of the flow past a circular cylinder performing a rotary oscillation. *J. Phys. Soc. Japan* **45**, 1038–1043.

TOKUMARU, P. T. & DIMOTAKIS, P. E. 1991 Rotary oscillation control of a cylinder wake. *J. Fluid Mech.* **224**, 77–90.

WEI, T. & SMITH, C. R. 1986 Secondary vortices in the wake of circular cylinders. *J. Fluid Mech.* **169**, 513–533.

WILLE, R. 1974 Generation of oscillatory flows. In *Flow-Induced Structural Vibrations* (ed. E. Naudascher), pp. 1–16. Springer.

WU, J., MO, J. & VAKILI, A. 1989 On the wake of a cylinder with rotational oscillations. *AIAA 2nd Shear Flow Conf., Tempe.*

ZDRAVKOVICH, M. M. 1982 Modification of vortex shedding in the synchronization range. *Trans ASME* I: *J. Fluids Engng* **104**, 513–517.